

Time Resolved Detailed Diagnostics to Characterize Step Fuel Composition Changes in a Lean Technically Premixed Hydrogen Enriched Flame

Ianko Chtereov^{1*}, Isaac Boxx¹

¹ Institut für Verbrennungstechnik, Deutsches Zentrum für Luft-und Raumfahrt (DLR), Stuttgart,
Germany

*ianko.chtereov@dlr.de

Abstract

Time resolved PIV and OH* chemiluminescence were employed to characterize step changes in fuel composition in lean, technically premixed swirl-stabilized methane flames. The fuel composition was quickly changed using a system of fast acting three-way valves and bypass lines from an initial 100% methane to 50/50% (by volume) methane/hydrogen mixture, while maintaining equivalence ratio and thermal power. The initial and final states of the combustor are characterized by similar flow-fields, a more compact flame with hydrogen enrichment, self-excited thermoacoustic fluctuations in pure methane flames, and lower amplitude thermoacoustic pulsation with hydrogen enrichment. Using proper orthogonal decomposition the dynamics of the heat release and velocity field are characterized during a thermoacoustic cycle in the initial condition and during the fuel composition transient. Toroidal vortices are observed to shed forced by the acoustic pressure, and the regions of maximum heat release seem to follow the vortices, suggesting that the vortices have a role in driving the thermoacoustic fluctuation. For these operating conditions, high hydrogen enrichment suppresses the thermoacoustic cycle during the settling period in the heat release signal from OH* chemiluminescence in the later part of the fuel composition transient.

1 Introduction

Combustion of hydrogen is increasingly relevant to industry as a means of chemical energy storage via hydrolysis from renewable power sources such as solar and wind, and as a means to reduce carbon emissions by power generation. One strategy of implementing hydrogen in industrial gas turbines is displacing some of the natural gas with hydrogen. The very different chemical properties of hydrogen present significant combustor design challenges. In particular, the higher flame speed and temperature of hydrogen imply that the flame will stabilize differently, have a different size and or shape, and exhibit different combustion dynamics. These different combustion physics affect combustor performance parameters such as hardware heat loading, combustor exit pattern factor, ignition and blowoff characteristics and pollutant emissions.

The effect of hydrogen-enrichment on the stability and emissions of premixed flames of methane and natural gas has been studied extensively with simplified model combustors (Zhang 2007, Liewen 2008a, Liewen 2008b, Ghoniem 2005, Taamallah 2015, Shanbhogue 2016). Researchers observed that hydrogen addition lowers the fuel/air equivalence ratio for extinction, changes the

extinction dynamics and can change the flame mode in flow fields with multiple flame stabilization locations. Thermoacoustic oscillations in combustors or combustion instabilities occur when the heat release and combustor acoustics couple. High amplitudes of these oscillations can cause immediate damage or shorten hardware life through increased thermal and mechanical stress, and are therefore highly undesirable. Hydrogen addition is also observed to change the combustion instability limits and dynamics.

Daily operation of gas turbine power plants can require switching of fuels and fuel composition and ramping up and down thermal load. Such changes are nominally gradual but sudden incidental changes can occur, such as compressor surge or stall, or accidental fuel cutoff. The implication on combustor performance during these transients is of interest to design engineers. Furthermore, it is of academic interest to study the evolution of flame curvature, flame surface density and flame stretch during sudden changes in fuel composition.

This study utilized time-resolved detailed laser diagnostics (PIV, PLIF, chemiluminescence and three-microphone acoustics) to experimentally characterize a step change in fuel composition of a swirl stabilized methane-air flame in a laboratory scale burner. The change forced the flame from pure CH₄ to 50/50% (by volume) H₂/CH₄ while holding constant the global equivalence ratio and thermal power. The experimental measurements are analyzed to help understand the dynamics of the heat release distribution, flow field, and combustion instabilities as this sudden change in fuel composition occurs.

2 Experiment Setup

Laboratory scale burner

Experimental studies were performed at atmospheric pressure in the technically premixed gas turbine model combustor shown in Figure 1(a), previously widely studied experimentally (Meier 2007, Steinberg 2013, Oberleithner 2015) and computationally (Fiorina 2010, Wang 2014, Franzelli 2012). The burner consists of a plenum, a swirled inflow injector, an optically accessible combustion chamber and a choked exhaust nozzle. Air first enters the plenum and then passes through a swirl generator with 12 radial vanes. Fuel is injected through 1mm orifices in the swirler. The swirling, technically premixed flow then enters the combustor chamber through a nozzle with an exit diameter of D = 27.85 mm. Centered within the nozzle is a conical centerbody. The combustion chamber has a square cross-section of 85 × 85 mm² and a height of 114 mm. Optical access to the chamber is provided by side walls made of quartz glass held by metal posts in the corners. The exhaust nozzle consists of a conical part followed by an exhaust duct with 40 mm inner diameter.

This study focuses on a flame with 20kW thermal load and equivalence ratio $\phi=0.85$ undergoing a sudden transition in fuel composition from 100% methane to 50/50 methane-hydrogen (by volume). The operating conditions are listed in Table 1. This sudden transition was accomplished via a pair of fast acting 3-way switching valves configured as shown in Figure 1(b). Initially, electromechanical mass flow controllers (MFCs) 1 and 2 feed a stream of pure methane to the burner, while MCF3 passes a stream of hydrogen to a piloted flare. Upon activation, the fast acting switching valves divert the methane flow from MFC2 to the flare and the hydrogen from MFC3 to the swirl flame. This ensures an impulse change in fuel composition and eliminates transients associated with the finite response time of the MFCs. The 15cm length of fuel hose between the switching valves and the burner results in a short burst of the remaining unmixed methane being

pushed out by the hydrogen/methane mixture due to the increased volume flow rate. This is discussed in more detail in the analysis and discussion section.

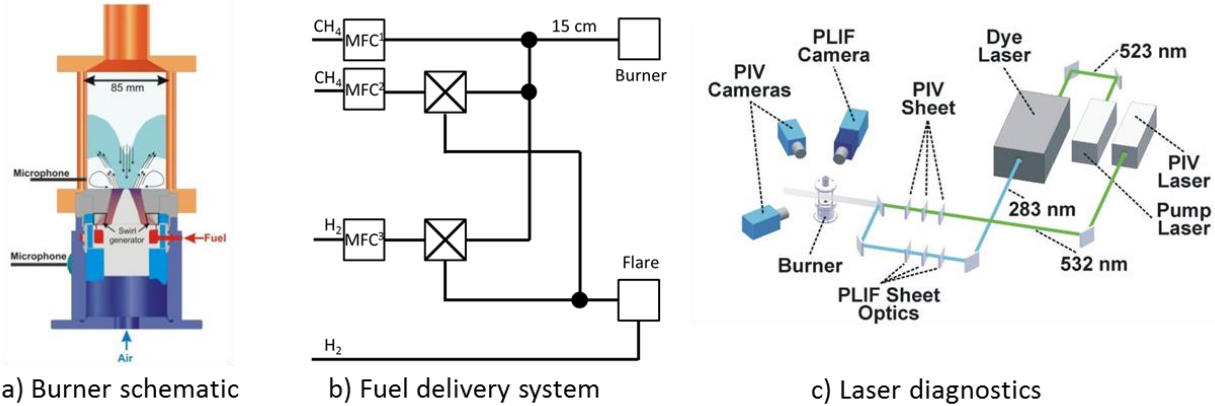


Figure 1: a) PRECCINSTA premixed swirl burner. The shape of the flame zone is indicated in the combustion chamber and the overall flow field is sketched. b) Fuel delivery system. c) Setup for the simultaneous high-speed OH PLIF/PIV/OH CL measurements at 10 kHz repetition rate.

High speed detailed diagnostics

Simultaneous, stereoscopic PIV and OH* chemiluminescence (CL) imaging was performed at a repetition rate of 10 kHz. OH* CL is a commonly applied marker for line-of-sight integrated heat-release. The experimental setup is depicted in Figure 1(c).

The OH* CL signal was collected with an intensified high-speed CMOS camera (LaVision HSS 5 with LaVision HS-IRO) equipped with a fast UV lens (Cerco, $f = 45$ mm, $f/D=1.8$) and a bandpass filter (300–325 nm). The intensifier gate time was 25 μ s.

The stereoscopic PIV system consisted of a dual-cavity Nd:YAG DPSS laser (Edgewave IS6II-DE) with a pulse energy of 2.6 mJ/pulse at 532 nm. The laser beam was expanded into a light sheet with a dual-stage cylindrical telescope and focused into the test section using a third cylindrical lens, resulting in a sheet with a height of approximately 40 mm and a thickness of approximately 1 mm. This laser sheet was aligned to pass approximately 2 mm above the combustor nozzle exit plane to reduce scattered light pollution. Mie scattering of titanium dioxide particles was imaged with a pair of high-speed CMOS cameras (LaVision HSS 8), equipped with commercial camera lenses (Tokina, $f = 100$ mm, set to $f/D=5.6$). Vector fields were computed from the particle images using a commercial PIV software (LaVision DaVis 8.0) with a multi-pass, adaptive window offset cross-correlation algorithm. The final interrogation window size was 16x16 pixels (corresponding to an in-plane spatial resolution of 1.0x1.0 mm²) with a window overlap of 50%.

Pressure in the chamber was measured using amplitude- and phase-calibrated microphone probes equipped with B&K Type 4939 condenser microphones. One probe was placed in the plenum, and another one in the combustion chamber at a height of $x = 15$ mm. The signals were recorded simultaneously using a multichannel A/D converter with a sampling rate of 100 kHz.

The OH* images were first dark field image corrected and then divided by a white field image (also dark field corrected), produced using a white screen, to compensate for the intensifier and lens non-

uniform spatial response. The acoustic pressure signals were calibrated using the phase and amplitude curve for each probe in frequency space.

Table 1: Operating conditions for the fuel composition switch sequence. Values marked with (*) are nominal and are affected by the fuel composition adjustment.

State	\dot{Q} [kW]	ϕ	% Vol. H ₂	p_{RMS} [Pa]	Time Range [ms]	f_1 [Hz]
“Unstable”	22	0.85	0	98	000-440	295
“Transient”	22*	0.85*	-	-	440-540	-
“Stable”	22	0.85	50	72	540-1000	419

3 Analysis and Discussion

As shown in Table 1, data are collected with 100% CH₄ for 440 ms before the fuel change takes effect, then after a transient the burner is operated with 50/50% by volume CH₄/H₂. This sequence of events is represented in Figure 2 as a time trace of the integrated OH* CL signal. From t=0 to t=440 ms (line 1), the OH* CL signal fluctuates as a result of the thermoacoustic instability. The FFT of the acoustic pressure for initial, thermoacoustically unstable state is shown in Figure 3 with 5 Hz resolution, blue curve. A sharp peak is seen at 295 Hz as noted in Table 1. In the OH* CL signal, from t=440 ms (line 1) onward there is a slight drop followed by a quick overshoot. The drop and overshoot are probably due the fuel system design. Referring back to Figure 1(b), as hydrogen is switched in from MFC3 to replace the methane from MFC2, some synchronization mismatch in the actuated 3-way valves combined with the fuel line lengths and fuel density differences could be causing the initial drop in heat release, while eventually the lower density of hydrogen and resulting increased volume flow rate through the line pushes out the remaining unmixed methane, corresponding to the overshoot. At t=490 ms (line 2) there is a settling period until t=540 ms (line 3), after which the combustor is observed to be acoustically stable. It can be seen in the red curve of Figure 3, there is a weaker peak at 419 Hz and the spectrum is much broader after the fuel composition shift. Within the stable combustion period there is some “adjustment” of the heat release as can be seen in steady drift up of the time trace in Figure 3 after line 3.

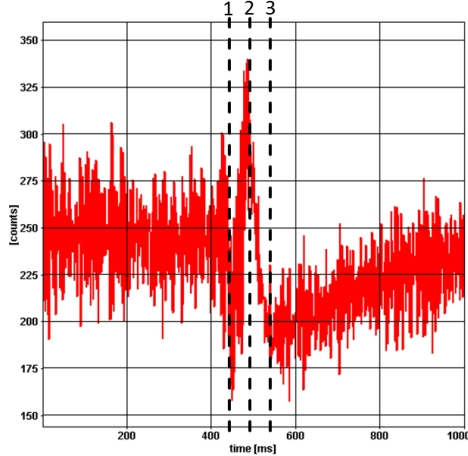


Figure 2: Time series of total heat release (full field integrated OH* chemiluminescence). The transition period is between lines 1 and 3.

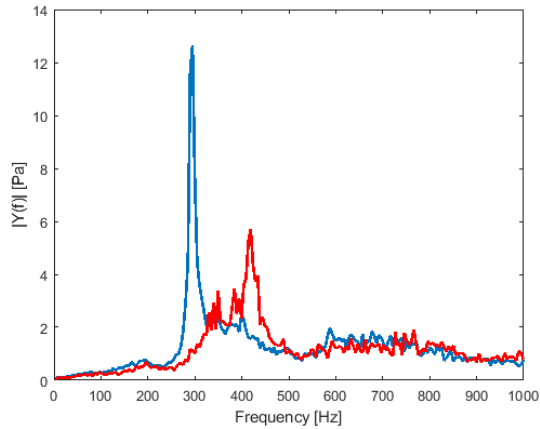


Figure 3: Acoustic pressure FFT with and without hydrogen enrichment (blue: 0% H₂, red: 50% H₂ by volume). 5 Hz spectral resolution.

We further characterize the initial and final state by examining the PIV and OH* CL data. Figure 4 shows the time-averaged OH* CL fields for the initial and final state – the frame ranges from Table 1 are used. Note that the same intensifier gate is used for the two states. Both states reveal a V-shaped, inner shear layer stabilized flame. The hydrogen-enriched flame shows a shorter, more intense flame compared to the initial, pure methane state. This may be attributed to the faster diffusion/chemistry and flame speed of the hydrogen-enriched fuel. This shortening of the flame has the potential of increasing hardware heat load due to the increased thermal power per volume, and can result in a stronger coupling of the flame and combustor acoustics at higher frequencies (shorter wavelengths).

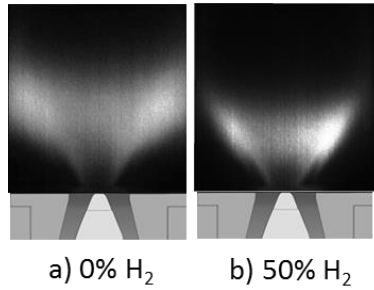


Figure 4: Time averaged OH* chemiluminescence images with and without hydrogen enrichment.

In Figure 5(c) streamlines from the time-averaged PIV fields are plotted. The basic topology of the flow-field is revealed: annular jet of ensuing fuel/air mixture, vortex breakdown with an inner and outer recirculation zones (IRZ/ORZ), separating inner shear layer between the annular jet and IRZ, and outer shear layer between the annular jet and ORZ. The flame for these operating conditions stabilizes primarily in the inner shear layer, but as shown previously (Meier 2007, Steinberg 2013, Oberleithner 2015) the flame can also stabilize in the outer shear layer at fuel leaner conditions and higher thermal power. The flow-fields of the methane only and hydrogen/methane mixture flames are qualitatively similar.

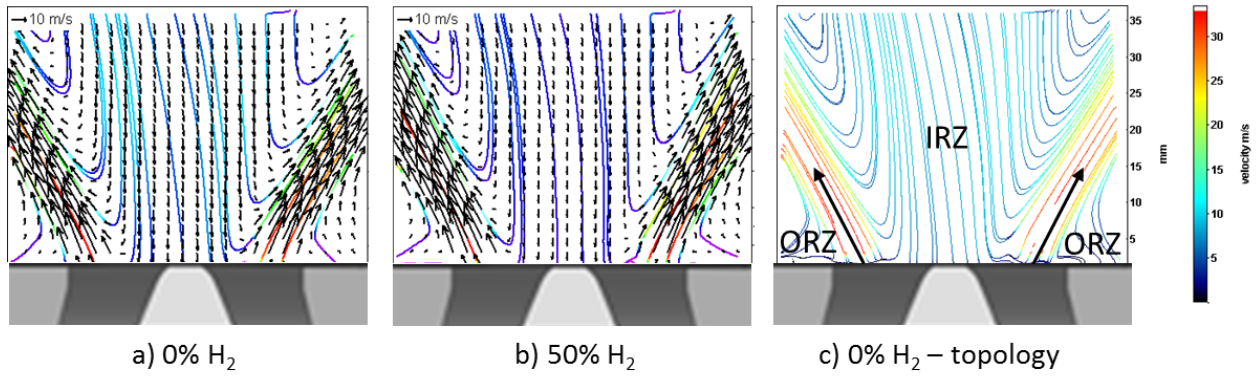


Figure 5: Time averaged PIV fields and streamlines with and without hydrogen enrichment.

Proper orthogonal decomposition (POD) is commonly used to quantify oscillatory flow dynamics. Turning to the dynamics of the fuel composition transient, POD is performed and presented here on the PIV and OH* CL fields for the transient period (see Table 1). Figure 6 contains (a) the first two spatial modes, (b) the first two temporal modes for the duration of the transition, and (c) the energy content of the first 10 modes. The spatial modes are displayed using streamlines to aid visualization. We focus on the first two modes as the spatial modes are highly symmetric and contain 8%+7%=15% of the energy. A reconstruction of the PIV fields using the first two modes (see Figure 8) also reveals the toroidal vortices driven by the acoustic field. Shear layer vortices are commonly induced in step expansion or annular combustors by the acoustic pressure of thermoacoustic fluctuations. These induced vortices have been observed to couple the acoustics and heat release by modifying the heat release by increasing flame area and/or interactions with the walls (see Gonzalez 2005, Renard 2000, Altay 2009). The higher POD modes are asymmetric and significantly weaker. The authors have verified that POD in the unstable, methane only period (see Table 1), produces very similar PIV and OH* CL spatial modes. Therefore, the discussion of the thermoacoustic dynamics is based on POD of the transient period.

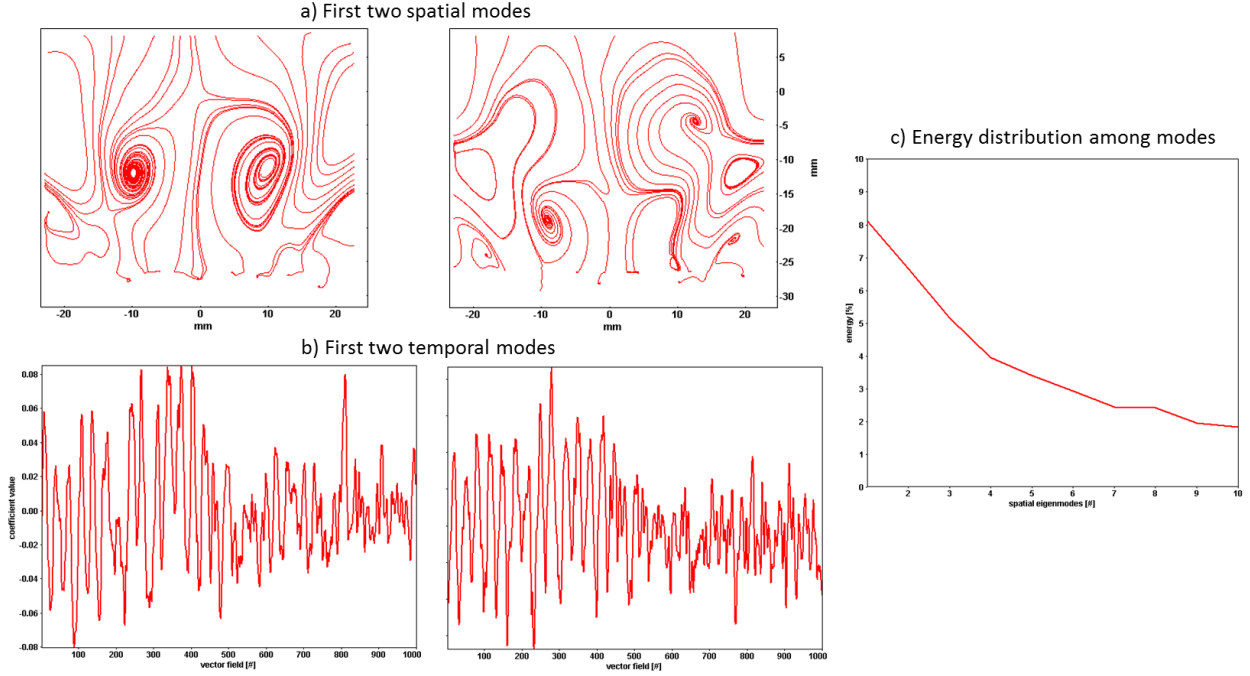


Figure 6: POD decomposition of PIV without hydrogen enrichment: a) streamlines of first two spatial modes, b) first two temporal modes during transient, c) energy distribution among the first 10 modes.

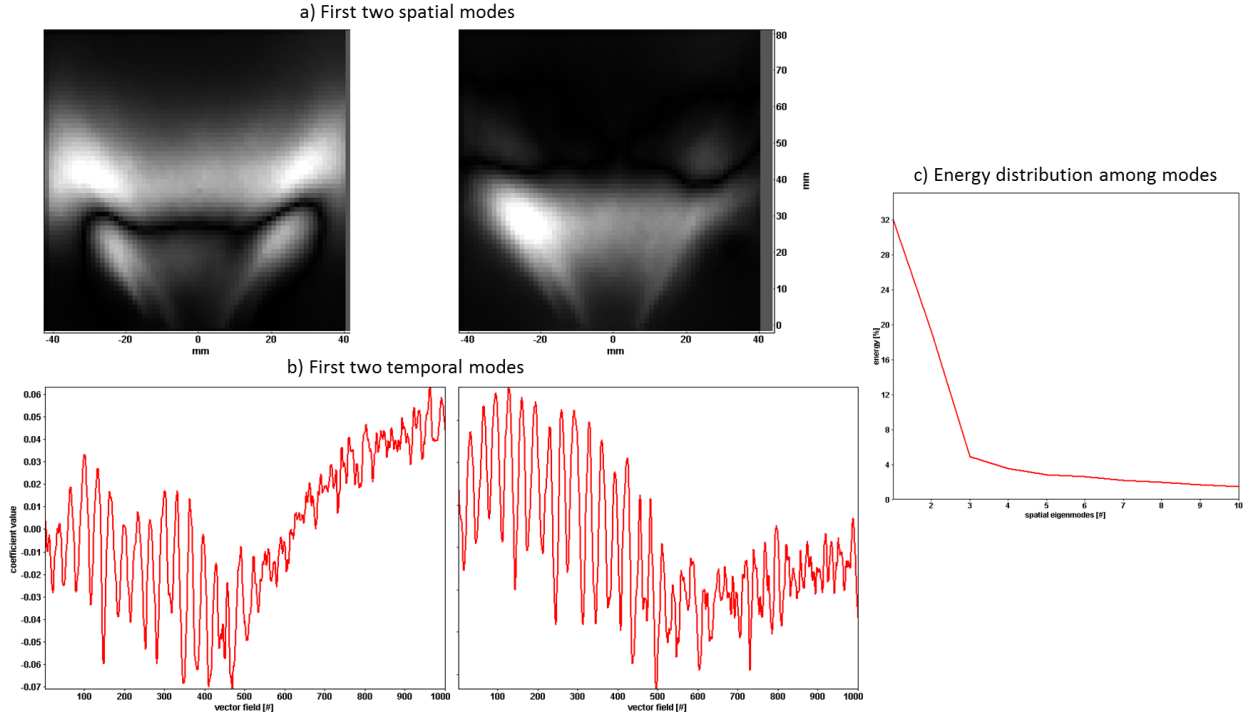


Figure 7: POD decomposition of OH chemiluminescence without hydrogen enrichment: a) streamlines of first two spatial modes, b) first two temporal modes during transient, c) energy distribution among the first 10 modes.

Figure 7 shows a similar treatment of the OH* CL fields. The first two modes of the OH* CL are obviously dominant as together they contain $32\%+28\%=60\%$ of the energy, with the third mode only containing 5% of the energy. POD reconstruction of the OH* CL fields using the first two modes is also shown in Figure 8.

Figure 8 shows an image sequence of 3.2 ms duration or approximately 340 degrees of the 295 Hz thermoacoustic pulsation cycle observable in flame prior to the fuel-composition change. At $t=0.0$ ms, a toroidal vortex is seen roughly in the middle of the PIV field of view. The vortex propagates downstream as time progresses. By time $t=2.4$ ms the vortex has moved out of the field of view and a new one is seen propagating up from the lower part of the measurement field of view. During the cycle the regions of maximum heat release seem to correlate well with the location of the toroidal vortices in the PIV fields, suggesting that flame-vortex interactions have an important role in the thermoacoustic cycle of the subject combustor.

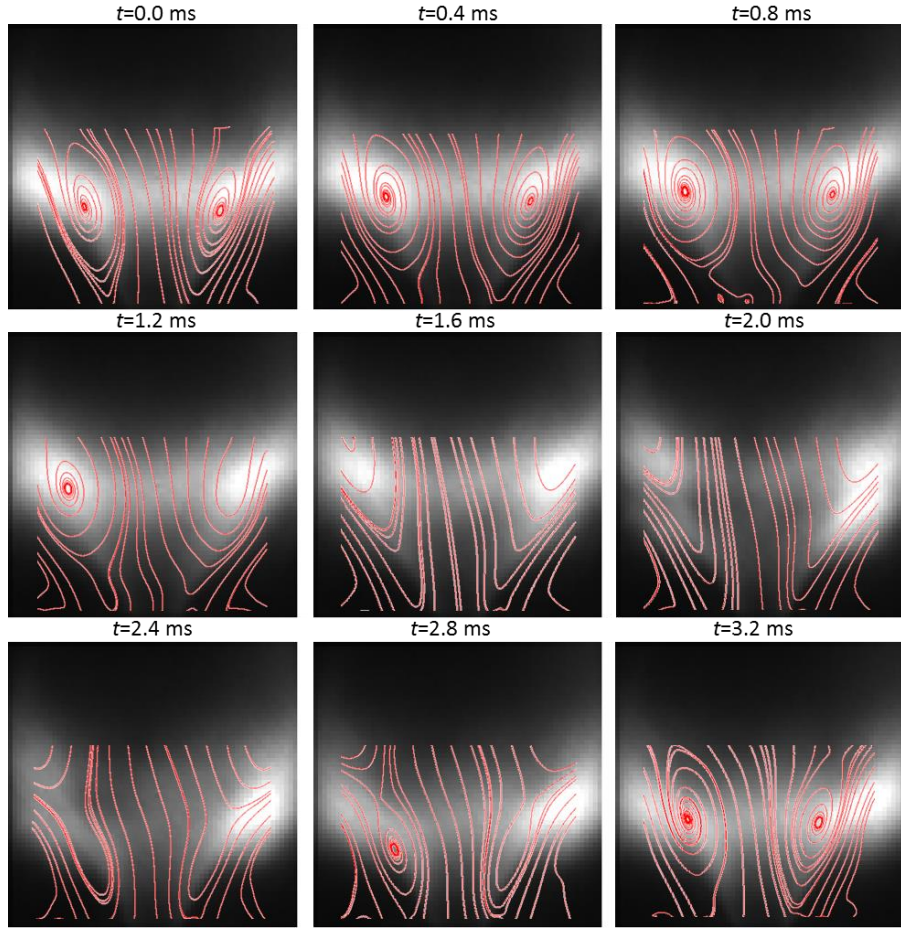


Figure 8: One thermoacoustic cycle: first two POD modes reconstruction of OH* chemiluminescence and PIV. PIV streamlines shown.

Turning our attention back on the fuel change transient, we examine the temporal modes in Figure 6 and Figure 7. The first two modes of both the PIV and OH* CL fields show fairly periodic behavior with a period consistent with the 3.4 ms period of the 295 Hz thermoacoustic frequency for the first

500 frames, or for about 50 ms of the transition period, corresponding to the drop and overshoot periods in the integrated heat release signal in Figure 2, between lines 1 and 2. The POD temporal modes in Figure 6 and Figure 7 of the thermoacoustic cycle are disrupted in the settling period between lines 2 and 3 in Figure 2, as evidenced by low periodicity in the POD modes after the first 500 frames or 50 ms of the transient period. Therefore, hydrogen enrichment in this case suppresses the thermoacoustic instability by changing the flame response and/or coupling mechanism. This is a somewhat counterintuitive result, with engineering relevance.

4 Concluding Remarks

Time resolved PIV and OH* chemiluminescence imaging are used to study the dynamics of the hydrogen enriched flame in the initial and final states, as well as during the transient period.

Toroidal vortices are observed to shed forced by the acoustic pressure, and the regions of maximum heat release seem to follow the vortices, suggesting that the vortices have a role in driving the thermoacoustic fluctuation. Also, at these operating conditions hydrogen enrichment suppresses the thermoacoustic cycle during the settling period in the heat release signal from OH* chemiluminescence in the later part of the fuel composition transient. Future work will incorporate simultaneous OH PLIF measurements to characterize the time evolution of flame curvature, and flame surface density.

Acknowledgements

This project has received funding from the European Research Council (ERC) under the European Union's Horizon 2020 research and innovation programme (Grant agreement No. 682383).

References

- Altay HM, Speth RL, Hudgins DE, and Ghoniem AF (2009) Flame–vortex interaction driven combustion dynamics in a backward-facing step combustor. *Combustion and Flame* 156(5) 1111:1125
- Fiorina B, Vicquelin R, Auzillon P, Darabiha N, Gicquel O, and Veynante D (2010) A filtered tabulated chemistry model for LES of premixed combustion. *Combustion and Flame* 157(3) 465:475
- Franzelli B, Riber E, Gicquel LY, and Poinsot T (2012) Large eddy simulation of combustion instabilities in a lean partially premixed swirled flame. *Combustion and flame* 159(2) 621:637
- Ghoniem AF, Annaswamy A, Park S, and Sobhani ZC (2005) Stability and emissions control using air injection and H₂ addition in premixed combustion. *Proceedings of the Combustion Institute* 30(2) 1765:1773
- Gonzalez E, Lee J, and Santavicca D (2005) A study of combustion instabilities driven by flame-vortex interactions. *41st AIAA/ASME/SAE/ASEE Joint Propulsion Conference & Exhibit* 4330
- Lieuwen T, McDonell V, Petersen E, and Santavicca D (2008) Fuel flexibility influences on premixed combustor blowout, flashback, autoignition, and stability. *Journal of engineering for gas turbines and power* 130(1) 011506
- Lieuwen T, McDonell V, Santavicca D, and Sattelmayer T (2008). Burner development and operability issues associated with steady flowing syngas fired combustors. *Combustion Science and Technology* 180(6) 1169:1192

- Meier W, Weigand P, Duan XR, and Giezendanner-Thoben R (2007) Detailed characterization of the dynamics of thermoacoustic pulsations in a lean premixed swirl flame. *Combustion and Flame* 150(1-2) 2:26
- Oberleithner K, Stöhr M, Im SH, Arndt CM, and Steinberg AM (2015) Formation and flame-induced suppression of the precessing vortex core in a swirl combustor: experiments and linear stability analysis. *Combustion and Flame* 162(8) 3100:3114
- Renard PH, Thevenin D, Rolon JC, and Candel S (2000) Dynamics of flame/vortex interactions. *Progress in energy and combustion science* 26(3) 225:282
- Shanbhogue SJ, Sanusi YS, Taamallah S, Habib MA, Mokheimer EMA, and Ghoniem AF (2016) Flame macrostructures, combustion instability and extinction strain scaling in swirl-stabilized premixed CH₄/H₂ combustion. *Combustion and Flame* 163 494:507
- Steinberg AM, Arndt CM, and Meier W (2013) Parametric study of vortex structures and their dynamics in swirl-stabilized combustion. *Proceedings of the Combustion Institute* 34(2) 3117:3125
- Taamallah S, Vogiatzaki K, Alzahrani FM, Mokheimer EMA, Habib MA, and Ghoniem AF (2015) Fuel flexibility, stability and emissions in premixed hydrogen-rich gas turbine combustion: Technology, fundamentals, and numerical simulations. *Applied energy* 154 1020:1047
- Wang P, Platova NA, Fröhlich J, and Maas U (2014). Large eddy simulation of the PRECCINSTA burner. *International Journal of Heat and Mass Transfer* 70 486:495
- Zhang Q, Noble DR, and Lieuwen T (2007). Characterization of Fuel Composition Effects in H₂/CO/CH₄ Mixtures Upon Lean Blowout. *Journal of engineering for gas turbines and power* 129(3) 688:694